Food Control 98 (2019) 174–178

Contents lists available at ScienceDirect

Food Control

journal homepage: www.elsevier.com/locate/foodcont

Porous metal-organic framework (MOF) Carrier for incorporation of volatile antimicrobial essential oil

Yunpeng Wu[a], Yaguang Luo[b,c], Bin Zhou[b], Lei Mei[a], Qin Wang[a], Boce Zhang[d,*]

[a] Department of Nutrition and Food Science, University of Maryland, College Park, MD, 20742, USA
[b] Environmental Microbial and Food Safety Lab, US Department of Agriculture, Agricultural Research Service, Beltsville Agricultural Research Center, Building 002, Beltsville, MD, 20705, USA
[c] Food Quality Lab, US Department of Agriculture, Agricultural Research Service, Beltsville Agricultural Research Center, Building 002, Beltsville, MD, 20705, USA
[d] Department of Biomedical and Nutritional Sciences, University of Massachusetts, Lowell, MA, 01854, USA

ARTICLE INFO

Keywords:
Metal-organic framework
Thymol
Antimicrobial property

ABSTRACT

The increasing demand for safety and quality in food products has stimulated research on developing natural preservatives and their carrier systems as a novel preventive control strategy. In this study, metal-organic framework (MOF) was investigated, for the first time, as a carrier for volatile antimicrobial essential oils. Zinc metal-organic framework (Zn@MOF) was synthesized with zinc nitrate hexahydrate and 2-aminoterephthalic acid in N, N-dimethylformamide (DMF). Thymol was then loaded into the Zn@MOF at a loading rate of 3.96% as measured by thermogravimetric analysis (TGA). The crystal structure of porous MOF was confirmed using scanning electron microscopy (SEM) and X-ray diffraction (XRD). Antibacterial activity of thymol loaded Zn@MOF (T-Zn@MOF) with active thymol loading of 0.029 g/100 g was assessed against a three-strain cocktail of *E. coli* O157:H7 in a tryptic soy broth (TSB). *E. coli* O157:H7 growth in T-Zn@MOF exhibited growth inhibition without an exponential growth phase after 24 h of incubation, which could be attributed to the sustained release of thymol by incorporating it in the porous Zn@MOF through noncovalent interactions. This research demonstrates that Zn@MOF loaded with the essential oil thymol is an effective antimicrobial and may have potential indirect applications in food.

1. Introduction

Growing demand for safe, high-quality foods with increased shelf-life has stimulated interest in developing food preservatives from natural antimicrobials, to improve food safety without sacrificing quality. For instance, one of the volatile essential oils found in thyme and oregano, thymol, has been identified as having antifungal, insecticidal, antibacterial, and antioxidant properties (Coimbra et al., 2011; Cristani et al., 2007). Because of the phenolic hydroxyl group on its structure, thymol is able to destroy the membrane of gram-negative bacteria and disturb the inorganic ion equilibrium and pH homeostasis inside the cytoplasm of prokaryotic cells (Pirbalouti, Rahnama, Malekpoor, & Broujeni, 2011). In addition, thymol binds to membrane proteins and intracellular targets, impairs the citrate metabolic pathway and interferes with enzymes involved in ATP synthesis, thus impeding cell recovery after brief exposure (Di Pasqua, Mamone, Ferranti, Ercolini, & Mauriello, 2010). Also, low concentrations of thymol inhibited the secretion of enterotoxins in *Staphylococcus aureus* (Qiu et al. 2010). These antimicrobial activities suggest that thymol could potentially be used as a food preservative. However, the application of thymol is limited due to two major drawbacks: undesirable aroma and low solubility in water. Various approaches to removing its strong unpleasant aroma, including temperature treatment (heat and refrigeration), decreasing redox potential, lowering water activity, and using other food additives have been reported (Burt, 2004). The other difficulty in thymol application is that its low solubility in water reduces its contact with bacteria in water, and therefore limits its inhibition efficacy. Development of micelles and nanoparticles to incorporate thymol are the main approaches to solve this limitation, as they promote better dispersion of thymol in water, as well as maximizing the surface area of the bacteria-thymol interaction. (Hu, Du, Wang, & Feng, 2009; Singh, Maurya, Catalan, & De Lampasona, 2004; Viuda-Martos et al., 2011; Yildirim, Kordali, & Yazici, 2011). In a previous study, we developed a method to incorporate thymol in zein nanoparticles to enhance its water solubility. The resulting zein-incorporated thymol maintained its antimicrobial activity against *E. coli* (Wu, Luo, & Wang, 2012). In this study, a new

* Corresponding author.
E-mail address: boce_zhang@uml.edu (B. Zhang).

https://doi.org/10.1016/j.foodcont.2018.11.011
Received 5 August 2018; Received in revised form 24 October 2018; Accepted 6 November 2018
Available online 07 November 2018
0956-7135/

approach is being exploited by using the metal-organic frameworks (MOFs) as the matrices to incorporate essential oils that have high volatility.

MOFs or porous coordination polymers have received much attention recently as a new class of hybrid materials that are formed by the self-assembly of metal-connecting ions and polydentate bridging ligands. In synthesizing MOFs, divalent (Zn^{2+}, Cu^{2+}) or trivalent (Al^{3+}, Cr^{3+}) metal cations are interconnected with the organic linker molecules to form polyhedral MOFs, resulting in molecular scale porous cavities (Jia, Yuan, & Ma, 2009; Sha et al., 2012). Using different organic linkers, the particle size, morphology and surface area can be modulated.

MOFs have either a crystalline or an amorphous structure, with the former attracting more interest due to its ordered structure and higher loading capacity for gaseous or volatile compounds (Sun, Qin, Wang, & Su, 2013; Wang et al., 2012). Applications of MOFs to date have been mostly limited to gas storage, catalysis, gas separation, and drug delivery (H.−C. Zhou, Long, & Yaghi, 2012). However, with recent success in synthesizing edible MOFs using γ-cyclodextrin and potassium ion (Smaldone et al., 2010), it is expected that MOFs could be applied in the food industries in the near future.

Comparing to other porous materials such as zeolite, MOFs have the following advantage. The nucleation and growth of MOFs can be achieved under relatively mild conditions (Hong, Hwang, Serre, Ferey, & Chang, 2009; Juan-Alcaniz, Gascon, & Kapteijn, 2012). In contrast, the preparation of zeolites usually requires high temperature (400 °C or higher) to remove the template. This limits the application of zeolites for embedding materials that are temperature-sensitive (e.g. bioactive compounds) and highly volatile (e.g. thymol).

In this study, we have demonstrated for the first time, a simple surfactant-free post-synthesis loading process of MOF with thymol. The antimicrobial activity of thymol loaded Zinc MOF (T-Zn@MOF) was evaluated against *E. coli* O157:H7 in liquid Tryptic Soy Broth (TSB) broth. Although still in the early stages of development, this proof-of-concept study of T-Zn@MOF as a novel application of a MOF for loading antimicrobials represents a potential breakthrough in the food safety field.

2. Materials & methods

2.1. Materials

Zinc nitrate hexahydrate (reagent grade), 2-aminoterephthalic acid (99%), chloroform (99.8%) and N,N-dimethylformamide (DMF, 99%) were purchased from Sigma-Aldrich (St. Louis, MO, USA). All the chemicals are analytical grade. Attenuated *E. coli* O157:H7, strain B6914/pGFP (ampicillin resistant) was purchased from American Type Culture Collection (ATCC; Manassas, VA), and tryptic soy broth (TSB) was acquired from Difco (Franklin Lakes, NJ).

2.2. Synthesis of Zn@MOF

The Zn@MOF was synthesized according to a previous report (Yoo, Varela-Guerrero, & Jeong, 2011). Zinc nitrate hexahydrate and 2-aminoterephthalic acid were dissolved in DMF separately to obtain a final concentration of 0.018 M (solution A) and 0.006 M (solution B), respectively. Both solutions were stirred vigorously for 1 h before mixing 10 mL of solution A and B together in a glass beaker. After sonication for 5 min, the solution was then processed solvothermally in a convective oven at 105 °C for 24 h. Afterward, the solution was cooled to the ambient temperature and centrifuged at 4193 g for 15 min to collect the Zn@MOF crystals. The crystals were then rinsed with fresh DMF three times. In order to remove the DMF inside the Zn@MOF pores, the freshly produced Zn@MOF was soaked in chloroform for 3 days with chloroform replenished every day. After thoroughly washing with chloroform, the dried Zn@MOF was obtained by overnight evaporation in the fume hood at ambient condition. The MOF was stored in a desiccator for further analysis.

2.3. Preparation of T-Zn@MOF

After collecting the dried Zn@MOF, thymol was loaded into the Zn@MOF pores by soaking overnight with stirring in sealed glass bottles containing 100 mg/mL of thymol in chloroform. Next, the thymol loaded Zn@MOF (T-Zn@MOF) was rinsed three times by centrifugation using fresh chloroform and the remaining solvents were evaporated in a fume hood overnight.

2.4. Characterization of Zn@MOF

2.4.1. Porosity and surface area

The porosity and surface area of Zn@MOF were determined using an ASAP 2020 Physisorption Analyzer (Micromeritics Instrument Corporation, Norcross, GA, USA). Sample tubes were cleaned ultrasonically and dried at 110 °C. The Zn@MOF was loaded into the sample tube by degassing for 24 h. The sample tube with Zn@MOF was then transferred to the analysis port with N_2 as the adsorptive gas and liquid nitrogen as the cold trap media.

2.4.2. Morphology and crystal structure

Scanning electron microscopy (SEM, SU-70 SEM, Hitachi, Pleasanton, CA, USA) was used to examine the morphology of Zn@MOF. Dried Zn@MOF crystals were adhered to conductive carbon tapes (Electron Microscopy Sciences, Ft. Washington, PA, USA), and mounted onto specimen stubs. The stubs were coated with a thin (< 20 nm) conductive gold and platinum layer by a sputter-coater (Hummer XP, Anatech, CA, USA). Digital images of the samples were obtained and representative images were reported.

X-ray powder Diffraction (XRD) patterns were obtained with an XRD diffractometer (C2 Discover Bruker Diffractometer, Madison, WI, USA) with CuKα radiation to evaluate the crystal structure of Zn@MOF.

2.4.3. Thermogravimetric analysis (TGA)

Thermogravimetric analyses were carried out using a TG 209 F3 instrument (Netzsch, Selb, Germany), starting at room temperature and going up to 250 °C with a heating rate of 10 °C per minute. Dual isotherms were programmed for 10 min at 100 °C to remove H_2O from T-Zn@MOF and 30 min at 250 °C to stabilize the mass. Samples (25 mg) were maintained in a nitrogen atmosphere. All analyses were performed in triplicate.

2.5. Inhibition of E. coli O157:H7 growth in liquid medium

Three-strain cocktails of *E. coli* O157:H7 with nalidixic acid resistance (FS4059, FS4066, and FS4076) were used in this study. A single colony for each strain was transferred to a tryptic soy broth (TSB, Neogen, Lansing, MI, USA) with 50 mg/L nalidixic acid (*E. coli*), and incubated for 20 h at 37 °C with shaking. Cells were harvested by centrifugation at 4300 g for 5 min, washed once in sterile phosphate-buffered saline (PBS), and re-suspended in PBS. Equal volumes of cell suspensions from each strain were mixed to achieve a cocktail of inoculum with approximately 10^9 CFU/mL, and diluted in PBS to achieve a cocktail of inoculum with approximately 10^6 CFU/mL. The inoculum was further transferred into TSB for the growth study.

Five treatments were tested in the growth study, including 1.) Control inoculation broth without MOF or thymol; 2.) Inoculation broth with 1 g Zn@MOF/100 g. 3.) Inoculation broth with 0.029 g thymol/100 g; 4.) Inoculation broth with 0.034 g thymol/100 g; 5.) Inoculation broth with T-Zn@MOF with active thymol loading of 0.029 g/100 g. All treatments were placed in a shaking incubator at 35 °C for 24 h. The optical density of each inoculated broth was measured at 600 nm.

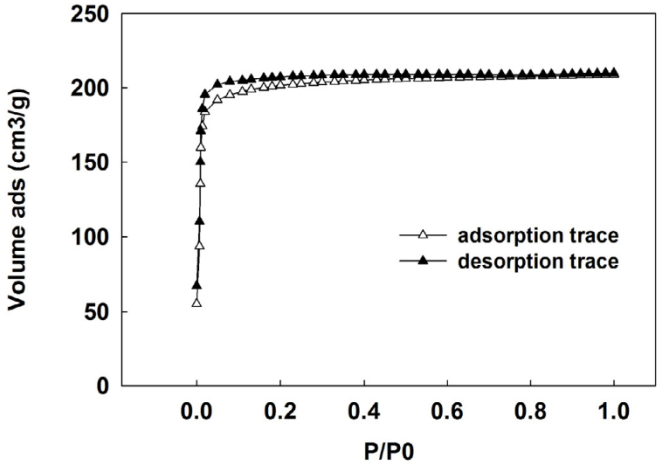

Fig. 1. N_2 isotherms (77 K) for Zn@MOF. Solid and empty triangles represent adsorption and desorption traces, respectively. The BET surface area is 617.53 m^2/g and pore size is 30.01 Å.

2.6. Statistical analysis

The data reported as mean ± standard error were from experiments conducted in triplicate. Experimental statistics were performed using a SAS software (Version 9.2, SAS Institute Inc., Cary, NC, USA). The analysis of variance (ANOVA) was used to compare the treatment means.

3. Results and discussion

3.1. Porosity and surface area

The N_2 adsorption-desorption isotherms of the Zn@MOF (Fig. 1) revealed the intraparticle porosity. The adsorption of N_2 increases logarithmically with the environmental pressure. The Brunauer–Emmett–Teller (BET) surface area (S_{BET}) of Zn@MOF was determined to be 617.53 m^2/g and the pore opening diameter was 30.01 Å. The specific surface areas of different types of MOFs are dependent on different metal ions and organic linkers. For example, MOF-5 is one of the most studied forms of MOF, and Au/ZnO@MOF-5 has the S_{BET} of 584 m^2/g (Mueller et al., 2011) and TiO_2@MOF-5 has the S_{BET} of 2,412 m^2/g (Muller, Zhang, Wang, & Fischer, 2009). The large surface area and pore diameter values were evidence for proving the porous structure of the MOF formed during the preparation of MOF (Yoo et al., 2011). These characteristics of the porous Zn@MOF suggest that it could hold a large number of thymol molecules (Chang, Bristowe, & Cheetham, 2013).

3.2. Morphology and crystal structures

SEM and XRD have been widely used to characterize different MOF structures. The morphology and crystal structure of MOFs can be studied by these two methods (Ploegmakers, Japip, & Nijmeijer, 2013; Y.-X.; Zhou et al., 2010).

SEM representative images of Zn@MOF were shown in Fig. 2. The crystalline Zn@MOF has a cuboid morphology, which is consistent with the reports of others (Z. Zhao, Xia, & Li, 2011). The dimension of Zn@MOF crystal is around 12 μm × 13 μm (Chen et al., 2010).

XRD patterns illustrate the MOF crystal structure at atomic and molecular level. Fig. 3 shows that the experimental pattern of Zn@MOF (blue line in Fig. 3) and its pattern calculated for body-centered cubic lattice (red line in Fig. 3) match very well. The best match was achieved by using the edge length of 18.36 Å, so the result from running the model suggests that the Zn@MOF is composed of body-centered cubic unit cells with the edge length of 18.36 Å. There was still some residual

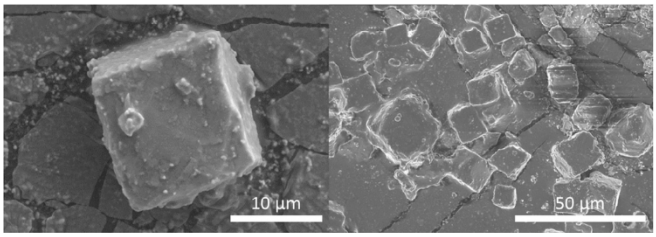

Fig. 2. SEM micrographs of Zn@MOF.

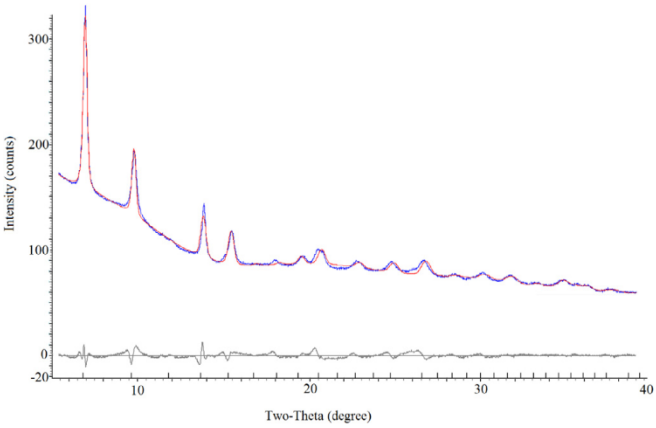

Fig. 3. XRD patterns of Zn@MOF. The blue line represents the experimental curve, and the red line shows the closest simulation with a cubic body centered lattice with a = 18.36 Å.

difference shown at the bottom in Fig. 3. This could be because 1) It is a distorted cubic lattice, e.g. in tetragonal or rhombohedral fashion; 2) There is another minor phase present that, for example, could be one of the multiple Zn nitrate compounds (F. H. Zhao, Che, & Zheng, 2012; Y.-X. Zhou et al., 2010). Unfortunately, due to the data quality (broad peaks and absence of high angle scattering), it is difficult to confirm the reason for this discrepancy.

3.3. Thermogravimetric analysis (TGA)

TGA is widely used to quantify the amount of material incorporated inside MOF, including surfactants (Yoo et al., 2011) and other reactants like $Zn(OH)_2$ (Chen et al., 2010). The TGA graph (Fig. 4) indicated that the weight loss took place in two temperature ranges: 20–100 °C and 100–250 °C. From the TGA plot, the first weight loss of 10.66% between 20 °C and 100 °C was assigned to the water desorption. Thymol incorporated inside T-Zn@MOF was evaporated between 100 and 250 °C, corresponding to a weight loss of 3.96% ± 0.03. According to the

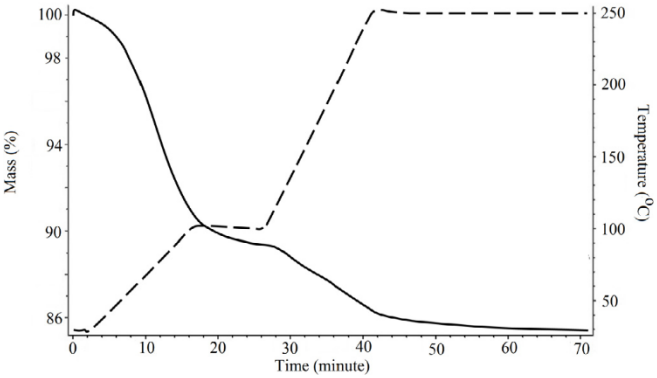

Fig. 4. Thermogravimetric analysis: solid and dashed lines represent thermogravimetry and temperature respectively.

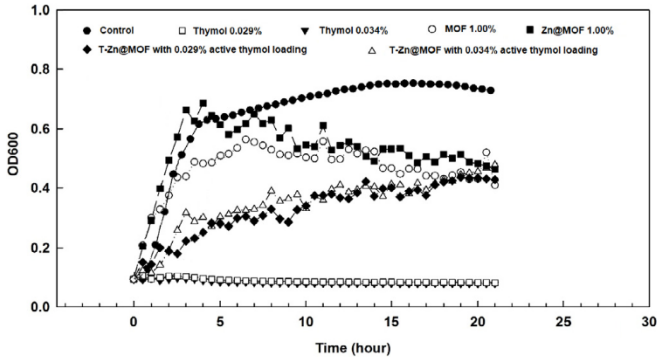

Fig. 5. Effect of T-Zn@MOF on the growth of three-stain cocktail of *E. coli* O157:H7. 1.) Control inoculation broth without MOF or thymol (solid circle); 2) Inoculation broth with thymol only with a loading rate of 0.029% (hollow square) and 0.034% (solid triangle). 3.) Inoculation broth with 1% of MOF (hollow circle) or Zn@MOF (solid square). 4.) Inoculation broth with 1% T-Zn@MOF with the active thymol loading of 0.029% (black diamond) and 0.034% (hollow triangle).

previous report, the decomposition of organic linker would take place at about 400 °C (Yoo et al., 2011). Therefore, the Zn@MOF was stable during the process of thermogravimetric measurement. All the thymol should be removed below 250 °C because the boiling point of thymol is 233 °C. Due to its volatility, thymol was expected to start to evaporate at around 150 °C (Shah, Ikeda, Davidson, & Zhong, 2012). Therefore, the T-Zn@MOF prepared in our study contained an average of 3.96% thymol.

3.4. Inhibition of E. coli O157:H7

The *in vitro* antimicrobial activity was evaluated by the comparison of the three-strain cocktail of *E. coli* O157:H7 in controls and T-Zn@MOF samples: 1.) Control inoculation broth without MOF or thymol; 2.) Inoculation broth with 1 g Zn@MOF/100 g. 3.) Inoculation broth with 0.029 g thymol/100 g; 4.) Inoculation broth with 0.034 g thymol/100 g (prepared by soaking Zn@MOF in 100 mg/mL thymol); 5.) Inoculation broth with T-Zn@MOF with active thymol loading of 0.029/100 g (prepared by soaking Zn@MOF in 10 mg/mL thymol).

As shown in Fig. 5, at the beginning of the exponential phase, Zn@MOF or MOF had no obvious inhibitory abilities, as the growth rate is very close to the control. After initial growth, no stationary phase was observed in the sample with Zn@MOF, which could be contributed to the low inhibitory effects of Zn ions in Zn@MOF. The two thymol samples with 0.034% and 0.029%wt loading rate showed strong bactericidal activities that no microbial growth was observed after 24 h of incubation. Although T-Zn@MOF treatment showed more microbial growth than thymol samples after 24 h, *E. coli* O157:H7 growth in the two T-Zn@MOF samples exhibited growth inhibition without exponential growth phase after 24 h of incubation. This could indicate the sustained release of thymol by incorporating it into the porous Zn@MOF through noncovalent interactions. Studies have shown that noncovalently bound materials can be released more easily from MOFs. Thymol is only slightly soluble in water (846 ± 9 ppm) (Griffin, Wyllie, Markham, & Leach, 1999; Wu et al., 2012) and the chance of its contacting bacteria is reduced by its poor solubility. Loading the thymol in Zn@MOF facilitated its separation and uniform diffusion in the incubation media, and also exhibited inhibitory effects again pathogenic bacteria.

4. Conclusions

Porous Zn@MOF was synthesized in this study. Its morphology, crystallinity, and porosity were characterized by XRD, SEM, and isotherm measurement, respectively. Furthermore, it was used for the incorporation of thymol for pathogen inhibition. T-Zn@MOF was demonstrated to be an effective antimicrobial against *E. coli* O157:H7 by achieving 4.4 Log reduction in 24 h. Further systemic evaluation on antimicrobial activities of the volatile discharge against multiple foodborne pathogens in food matrices is recommended to validate MOF's full potential as a carrier of volatile antiseptics for indirect food applications. Further studies may include exploring novel mechanisms of indirect and contract-free deployment of the material by fully exploiting the volatility of the entrapped bioactive ingredients in the MOF matrices. In addition, further investigation of the indirect or contact-free application of volatile essential oil using MOF as the delivery matrices requires a holistic evaluation of its antimicrobial efficiency on solid and liquid food, impact on aroma and flavor profile, as well as stability and sustained release profile of the volatile bioactive ingredients.

Acknowledgement

This project is supported by U.S. Department of Agriculture - National Institute of Food and Agriculture Award No. 2016-51181-25403 and U.S. Department of Agriculture-Agricultural Research Service Specific Corporative Agreement No. S51600000035794.

References

Burt, S. (2004). Essential oils: Their antibacterial properties and potential applications in foods - a review. *International Journal of Food Microbiology, 94*(3), 223–253.
Chang, B. K., Bristowe, P. D., & Cheetham, A. K. (2013). Computational studies on the adsorption of CO2 in the flexible perfluorinated metal-organic framework zinc 1,2-bis (4-pyridyl)ethane tetrafluoroterephthalate. *Physical Chemistry Chemical Physics, 15*(1), 176–182.
Chen, B., Wang, X. J., Zhang, Q. F., Xi, X. Y., Cai, J. J., Qi, H., et al. (2010). Synthesis and characterization of the interpenetrated MOF-5. *Journal of Materials Chemistry, 20*(18), 3758–3767.
Coimbra, M., Isacchi, B., van Bloois, L., Torano, J. S., Ket, A., Wu, X. J., et al. (2011). Improving solubility and chemical stability of natural compounds for medicinal use by incorporation into liposomes. *International Journal of Pharmaceutics, 416*(2), 433–442.
Cristani, M., D'Arrigo, M., Mandalari, G., Castelli, F., Sarpietro, M. G., Micieli, D., et al. (2007). Interaction of four monoterpenes contained in essential oils with model membranes: Implications for their antibacterial activity. *Journal of Agricultural and Food Chemistry, 55*(15), 6300–6308.
Di Pasqua, R., Mamone, G., Ferranti, P., Ercolini, D., & Mauriello, G. (2010). Changes in the proteome of *Salmonella enterica*serovar Thompson as stress adaptation to sublethal concentrations of thymol. *Proteomics, 10*(5), 1040–1049.
Griffin, S. G., Wyllie, S. G., Markham, J. L., & Leach, D. N. (1999). The role of structure and molecular properties of terpenoids in determining their antimicrobial activity. *Flavour and Fragrance Journal, 14*(5), 322–332.
Hong, D.-Y., Hwang, Y. K., Serre, C., Ferey, G., & Chang, J.-S. (2009). Porous chromium terephthalate MIL-101 with coordinatively unsaturated sites: Surface functionalization, encapsulation, sorption and catalysis. *Advanced Functional Materials, 19*(10), 1537–1552.
Hu, Y., Du, Y. M., Wang, X. Y., & Feng, T. (2009). Self-aggregation of water-soluble chitosan and solubilization of thymol as an antimicrobial agent. *Journal of Biomedical Materials Research Part A, 90A*(3), 874–881.
Jia, C., Yuan, X., & Ma, Z. (2009). Metal-organic frameworks (MOFs) as hydrogen storage materials. *Progress in Chemistry, 21*(9), 1954–1962.
Juan-Alcaniz, J., Gascon, J., & Kapteijn, F. (2012). Metal-organic frameworks as scaffolds for the encapsulation of active species: State of the art and future perspectives. *Journal of Materials Chemistry, 22*(20), 10102–10118.
Mueller, M., Turner, S., Lebedev, O. I., Wang, Y., van Tendeloo, G., & Fischer, R. A. (2011). Au@MOF-5 and Au/MOx@MOF-5 (M = Zn, Ti; x=1, 2): Preparation and microstructural characterisation. *European Journal of Inorganic Chemistry,* (12), 1876–1887.
Muller, M., Zhang, X. N., Wang, Y. M., & Fischer, R. A. (2009). Nanometer-sized titania hosted inside MOF-5. *Chemical Communications,* (1), 119–121.
Pirbalouti, A. G., Rahnama, G. H., Malekpoor, F., & Broujeni, H. R. (2011). Variation in antibacterial activity and phenolic content of Hypericum scabrum L. populations. *Journal of Medicinal Plants Research, 5*(17), 4119–4125.
Ploegmakers, J., Japip, S., & Nijmeijer, K. (2013). Mixed matrix membranes containing MOFs for ethylene/ethane separation Part A: Membrane preparation and characterization. *Journal of Membrane Science, 428*, 445–453.
Shah, B., Ikeda, S., Davidson, P. M., & Zhong, Q. X. (2012). Nanodispersing thymol in whey protein isolate-maltodextrin conjugate capsules produced using the emulsion-evaporation technique. *Journal of Food Engineering, 113*(1), 79–86.
Sha, J.-Q., Sun, J.-W., Wang, C., Li, G.-M., Yan, P.-F., & Li, M.-T. (2012). Syntheses study of Keggin POM supporting MOFs system. *Crystal Growth & Design, 12*(5), 2242–2250.
Singh, G., Maurya, S., Catalan, C., & De Lampasona, M. P. (2004). Chemical constituents,

antifungal and antioxidative effects of ajwain essential oil and its acetone extract. *Journal of Agricultural and Food Chemistry, 52*(11), 3292–3296.
Smaldone, R. A., Forgan, R. S., Furukawa, H., Gassensmith, J. J., Slawin, A. M. Z., Yaghi, O. M., et al. (2010). Metal-organic frameworks from edible natural products. *Angewandte Chemie international Edition, 49*(46), 8630–8634.
Sun, C. Y., Qin, C., Wang, X. L., & Su, Z. M. (2013). Metal-organic frameworks as potential drug delivery systems. *Expert Opinion on Drug Delivery, 10*(1), 89–101.
Viuda-Martos, M., Mohamady, M. A., Fernandez-Lopez, J., Abd ElRazik, K. A., Omer, E. A., Perez-Alvarez, J. A., et al. (2011). In vitro antioxidant and antibacterial activities of essentials oils obtained from Egyptian aromatic plants. *Food Control, 22*(11), 1715–1722.
Wang, C., Sun, L. G., Lv, L. L., Ni, L., Wang, S. H., & Yan, P. F. (2012). Study of the first POM columns pillared MOFs derivative. *Inorganic Chemistry Communications, 18*, 75–78.
Wu, Y., Luo, Y., & Wang, Q. (2012). Antioxidant and antimicrobial properties of essential oils encapsulated in zein nanoparticles prepared by liquid-liquid dispersion method. *LWT-Food Science and Technology, 48*(2), 283–290.
Yildirim, E., Kordali, S., & Yazici, G. (2011). Insecticidal effects of essential oils of eleven plant species from lamiaceae on Sitophilus granarius (L.) (Coleoptera: Curculionidae). *Romanian Biotechnological Letters, 16*(6), 6702–6709.
Yoo, Y., Varela-Guerrero, V., & Jeong, H.-K. (2011). Isoreticular metal-organic frameworks and their membranes with enhanced crack resistance and moisture stability by surfactant-assisted drying. *Langmuir, 27*(6), 2652–2657.
Zhao, F. H., Che, Y. X., & Zheng, J. M. (2012). Two metal-organic frameworks (MOFs) based on binuclear and tetranuclear units: Structures, magnetism and photo-luminescence. *Inorganica Chimica Acta, 384*, 170–175.
Zhao, Z., Xia, Q., & Li, Z. (2011). Role of temperature in the structure of Zn(II)-1,4,-BDC metal-organic frameworks and their adsorption and diffusion properties for carbon dioxide. *Separation Science and Technology, 46*(8), 1337–1345.
Zhou, Y.-X., Liang, S.-G., Song, J.-L., Wu, T.-B., Hu, S.-Q., Liu, H.-Z., et al. (2010). Synthesis of asymmetrical organic carbonates catalyzed by metal organic frameworks. *Acta Physico-chimica Sinica, 26*(4), 939–945.
Zhou, H.-C., Long, J. R., & Yaghi, O. M. (2012). Introduction to metal-organic frameworks. *Chemical Reviews, 112*(2), 673–674.